SCIENTIFIC REPORTS

OPEN

SUBJECT AREAS:
NANOPARTICLES
ELECTRICAL AND ELECTRONIC ENGINEERING
SELF-ASSEMBLY
SUSTAINABILITY

Received
22 April 2013

Accepted
8 August 2013

Published
2 September 2013

Correspondence and requests for materials should be addressed to X.W. (WANG.Xi2@nims.go.jp; wangxicas@gmail.com) or D.G. (GOLBERG.Dmitri@nims.go.jp)

Co_3O_4 nanocages with highly exposed {110} facets for high-performance lithium storage

Dequan Liu[1,2], Xi Wang[1], Xuebin Wang[1], Wei Tian[1], Yoshio Bando[1] & Dmitri Golberg[1]

[1]World Premier International (WPI) Center for Materials Nanoarchitectonics (MANA), International Center for Young Scientists (ICYS), National Institute for Materials Science (NIMS), Namiki 1-1, Tsukuba, Ibaraki 305-0044, Japan, [2]School of Physical Science and Technology, Key Laboratory for Magnetism and Magnetic Materials of the Ministry of Education, Lanzhou University, Lanzhou, 730000, China.

Functional materials with both exposed highly reactive planes and hollow structures have attracted considerable attentions with respect to improved catalytic activity and enhanced electrochemical energy storage. Herein, we report the synthesis of unusual single-crystal Co_3O_4 nanocages with highly exposed {110} reactive facets via a one-step solution method. When tested as anode materials in lithium-ion batteries, these Co_3O_4 nanocages deliver a high reversible lithium storage capacity of 864 mAh g^{-1} at 0.2C over 50 cycles and exhibit an excellent rate capability. The dominantly exposed {110} planes, a high density of atomic steps in nanocages, and the large void interiors lead to the regarded superior electrochemical performance.

Over the past few years, design and synthesis of nanostructures with exposed highly reactive crystal planes have great potentials for many applications such as new catalysts, and electrochemical energy storage[1–5]. Among them, Co_3O_4 nanocrystals with highly reactive facets have been paid more and more attentions due to their many promising properties. For example, a breakthrough has been made through the synthesis of Co_3O_4 nanorods with 41% high energy {110} exposed facets. The materials showed surprisingly high catalytic activity for CO oxidation at temperatures as low as $-77^{\circ}C$[6]. In addition, Li and coworkers[7] systematically studied the relationship between crystal plane structures of Co_3O_4 and their Li ion storage performance, and observed that Co_3O_4 nanooctahedrons with {111} planes showed better cyclic and rate properties than nanocubes with {001} planes. It was also reported that a high capacity of 380 $mAhg^{-1}$ at a high current density of 1000 mAg^{-1} can be delivered by a Co_3O_4 nanomesh with exposed {112} high energy facets[8]. In principle, (110) facet for Co_3O_4 nanocrystals is desirable for lithium-ion batteries (LIBs) when compared with (001) and (111) planes, because the former not only contains 2 Co^{3+} in one unit cell, but also more Co^{2+} ions (2.5 Co^{2+}) than the latter two planes (1.875 Co^{2+} for (111) and 1 Co^{2+} for (001)). However, highly reactive {110} facets for Co_3O_4 nanocrystals usually have high surface energy, and thus are hard to be prepared in the equilibrium state or via the traditional methods.

Notably, hollow nanostructures have also been actively explored in recent years due to their unique properties and applications specially related to anode materials in LIBs[9–13]. For instance, a hollow structured Co_3O_4 phase has high theoretical capacity (890 $mAhg^{-1}$), three times larger than the theoretical capacity of currently used graphite (<372 $mAhg^{-1}$); and hollow interior can effectively buffer the large volume changes during Li insertion-deinsertion, enables enhanced lithium storage performances[14–16]. In realistic state if Co_3O_4 materials not only have the exposed {110} high energy facets but also hollow features, their electrochemical performance is believed to be greatly improved. Such ideal architecture can simultaneously provide: (1) more active Co atoms on the surface and an improved ion diffusion rate within Co_3O_4 resulting from {110} plane effect, (2) structural stability due to hollow shell. However, this unique architectures for Co_3O_4 have not been achieved, because it requires that the shape of as-made Co_3O_4 must not be the traditional polycrystalline hollow sphere but unusual single-crystal polyhedral nanocage.

Herein, we developed a new one-pot strategy to synthesize Co_3O_4 unusual single-crystal nanocages with dominantly exposed {110} facets. Surprisingly a high density of atomic steps is found to be produced at the edges of these nanocages. To the best of our knowledge, it is the first report on fabrication of this kind of Co_3O_4 nanocages. When used as anode materials in LIBs, as-made nanocages exhibit excellent cycling performance and rate capabilities. They deliver a high reversible lithium storage capacity of 864 mAh g^{-1} at 0.2C over 50 cycles, near to theoretical capacity of Co_3O_4 (890 mAh g^{-1}). The enhancement of electrochemical performance can be

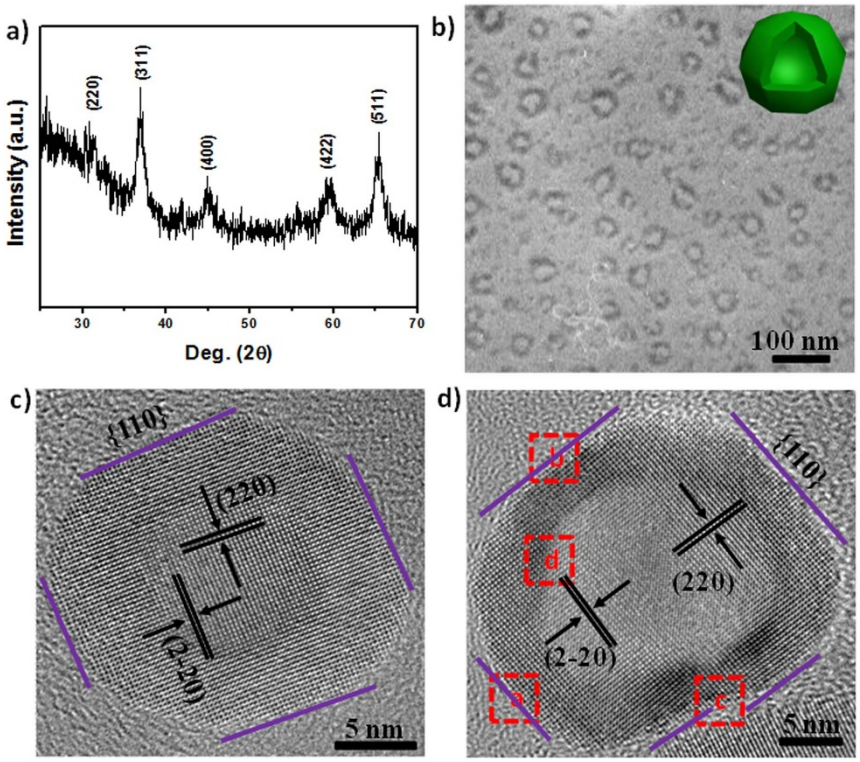

Figure 1 | Phase and Morphology analysis of Co_3O_4 hollow nanocages. (a) XRD pattern of single-crystal Co_3O_4 hollow nanocages (CoNs), (b) Low-magnification TEM image of CoNs. Inset showing the schematic drawing of a polyhedral nanocage. (c–d) HRTEM images of a single CoNs, the purple lines denote the exposed {110} facets.

attributed to the highly exposed {110} planes, a high density of atomic steps on surfaces, and the large void interiors.

Results

Characterization of Co_3O_4 nanocages with highly exposed {110} facets. The products were obtained after heat treatment of a mixed solution containing the cobalt glycolate (Fig. S1–S3, Supporting Information)[14] and H_2O_2 accompanied by a constant stirring. X-ray powder diffraction (XRD) patterns (Fig. 1a) demonstrate that the samples have identical peaks, which can be perfectly indexed to a pure Co_3O_4 (JCPDS card no. 42-1467)[14]. The broader peak implies the small size of the obtained products. Figure 1b shows a general morphology of Co_3O_4 products, in which the obvious contrast between the dark edge and pale center indicates their hollow nature. The size of resulting hollow particles is relatively uniform (~25 nm). High-resolution TEM (HRTEM) images of an individual product provide further insights into the structures and morphologies. As shown in Figures 1c–d, some relatively regular/flat edges are found in these capsules, that indicates that the shape of samples is not spherical, but unusual polyhedral. Although it is difficult to figure out the exact polyhedral morphology for each particle due to the plasticity and randomness of bubble soft templates used in this work, here we arbitrarily depict a schematic drawing of these unusual polyhedral nanocages (inset Fig. 1b). In addition, the hollow nanocages (CoNs) exhibit single-crystalline nature. As observed from Figures 1c–d, two sets of square crossing 2.8 Å fringes agree well with the {220} lattice spacing of *fcc* Co_3O_4[17] and its thickness is ~2–5 nm. From the edges of nanocages shown in Figures 1c–d, one can see that there are four sets of spacious {110} plane terraces. This suggests that {110} is the primarily exposed plane.

Another important feature of CoNs is that there are many zig-zag interfaces in both exteriors and interiors of nanocages (Fig. 1c–d, Fig. 2). It demonstrates that high energy facets may be present on their surfaces, and further suggests that the resulting products are indeed with unusual polyhedral architecture. It is because the unusual polyhedral structure can provide more freedom to produce kink interfaces (or atomic steps) than spherical or regular polyhedral ones. As revealed in Figure 2, surfaces of CoNs are terminated by a high density of atomic steps. Fig. 2a–c shows the exterior surfaces of the shell, in which a very high density of atomic steps and kinks for

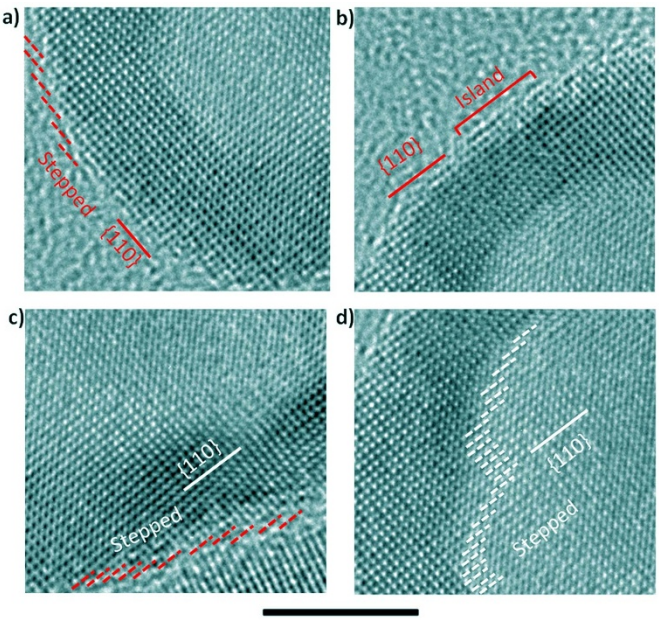

Figure 2 | Structure analysis of the edges of Co_3O_4 hollow nanocages. HRTEM images taken from areas labeled with squares in Figure 1d: (a–c) The outer shell of CoNs, (d) The inner shell of CoNs. Scale bar: 5 nm.

both convex and concave curvatures is frequently observed. For example, only a small piece of the surface in site ***a*** taken from Figure 1d, shown in Figure 2a, is composed of 7 terraces separated by atomic steps. Even in some flat surfaces, monoatomic-layer islands can always be found. For example, as observed in Figure 2b, a 3 nm island locates on a flat (110) terrace, which is probably stabilized by the out-of-plane convex curvature of the CoNs. In addition, the curved surfaces with a high density of atomic steps and kinks can also be seen from the concave curvatures, as depicted in Figure 2c. Note that the general feature of the (110)-terminated facets is that the non-ordered terraces are always seen (Fig. 2a–c). This may be consistent with their higher surface free energies, when compared with (111) plane ($\gamma_{(110)} = 2.561\ Jm^{-2}$, $\gamma_{(111)} = 0.974\ Jm^{-2}$)[18,19]. We also investigate the interior region of the hollow nanocages. As illustrated in Figure 2d, their internal surfaces involve a complex arrangement of {110} surfaces and a significant number of kinks within the surface steps. Generally, the presence of a high density of atomic steps has been predicted to be one of the important origins of the high catalytic activity of small nano-catalysts[20–22]. Similarly, this feature may facilitate the enhancement of the electrochemical performance of Co_3O_4.

The possible formation mechanism. Formation process of the CoNs products was further investigated at different reaction stages. After the initial reaction time (10 min), dot-like Co_3O_4 nanoparticles (Fig. 3a, Fig. S4, Supporting Information) in the size range of ~3–6 nm were produced via a heat-driven decomposition of the cobalt glycolate compound[14]. When the reaction time increased upto 30 min, several as-made nanoparticles would aggregate together. As observed in Figure 3b, five nanocrystals are recognized to gather together, because the shadow (size and shape) of the original particles, as well as their crystalline orientation, is visible. Note that as-prepared product at this stage showed a curled morphology and holes in it. Finally, these assemblies transformed into single-crystalline nanocages after continuous heating for 2–5 h. As mentioned previously, the resulting products showed four remarkable structural characteristics: highly exposed {110} planes, hollow interior, unusual polyhedral shape, and single-crystal.

Our results strongly support the idea that both the assembly of ethylene glycol (EG, from precursors, Fig. S3, Supporting Information) on the {100} surfaces and the presence of bubble templates play the important roles in the formation of the present structures, as illustrated in Figure 3c. Firstly, similar to the reported assemblies with cubic structures[23,24], EG molecules as the complexing agents may densely cover the surface of the {100} nuclei and thus ~3–6 nm nanoparticles are obtained. Packing EG on the {100} planes may be partly proofed by the fact that the nanocrystal fusion or growth towards <110> not <100> axes. As revealed in inset HRTEM image in Figure 3a, an angle of 135° can be identified, which indicates the presence of {110} surface planes. A reasonable model for such a small crystallite is depicted in the inset of Figure 3a. In consequence it leads to the exposed highly reactive {110} surfaces for nanoparticles and also for final nanocages. On the other hand, O_2-containing bubble templates released from H_2O_2 according to the reaction shown in Figure 3c, may also take effect. The bubble-like soft templates can partly be evidenced by formation of many cracked shells in final products (Fig. 1b, Fig. S5, see Supporting Information). As a result, in order to further minimize the whole system energy, several nanocrystals gather together on the surface of bubbles and thus the curled frameworks form (Fig. 3b), and these structures

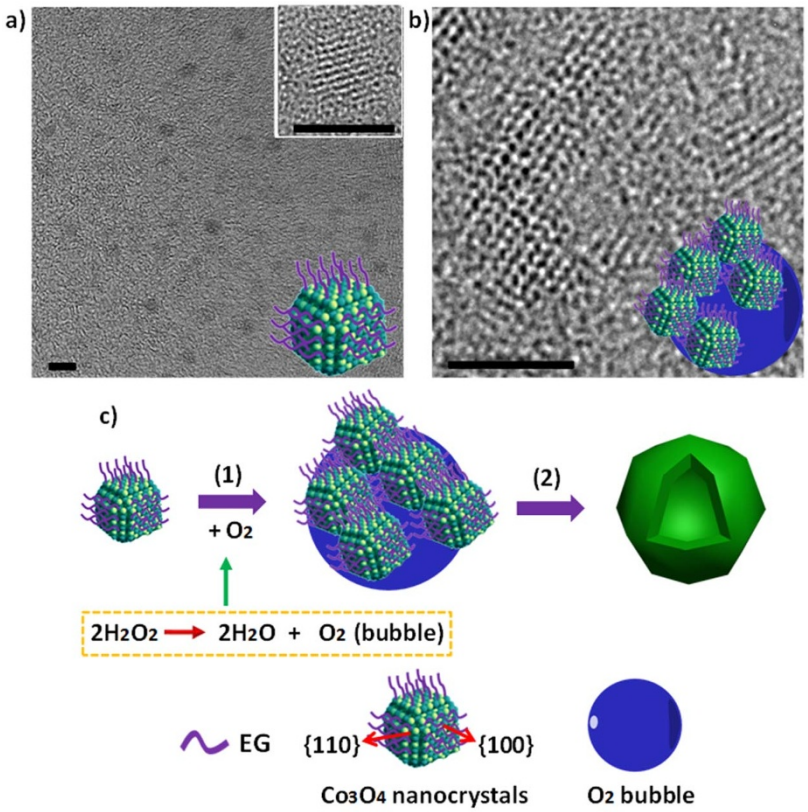

Figure 3 | Formation process of Co_3O_4 nanocages. (a) TEM image of ultra-small Co_3O_4 nanoparticles at early stages of the reaction (10 min). The inset shows a single nanoparticle and model structure of a truncated cuboctahedral shape. (b) HRTEM image of a product composed of nanoparticles at the following reaction stage (30 min). The inset shows schematic illustration of arrangement of several nanoparticles on the bubble surface. Note that some holes are observed. (c) Schematic illustration of the formation process of a single-crystalline hollow nanocage from small Co_3O_4 nanoclusters. The inset depicts the reaction forming O_2-containing bubbles. The scale bar: 5 nm.

seem to be unstable and then undergo surface reconstruction, resulting in single-crystalline hollow nanocages (Fig. 1c). It is worth noting that the average thickness of as-made CoNs is thinner than the original building blocks by up to 10–30%. That is because the diffusion and accommodation of the atoms under favorable thermodynamic conditions will occur in the rebuilding process. It also demonstrates that only few-layered (e.g. monolayer) building blocks can be placed on the surface of bubbles, which may be related to the strains within them. As for the formation of unusual polyhedral morphology, it may be associated with the flexibility of bubble soft template and aggregation modes of nanocrystals. In brief, unusual polyhedral nanocages with dominantly exposed {110} planes and high concentration of atomic steps are successfully synthesized via a feasible method. In contrast, only solid aggregates consisting of nanocrystals (Fig. S6, Supporting Information) formed in the absence of H_2O_2. From this point of view, hollowing is not only driven by minimizing high-energy surfaces, but also dependent on the soft templates.

Electrochemical properties of Co_3O_4 nanocages for lithium storage. The electrochemical performance of the samples was evaluated by using the standard half-cell. Figure 4a shows the 1st, 2nd, 10th, 30th, and 50th cycle discharge-charge voltage profiles for CoNs at a current density of 0.2C. The curves are characteristic of a Co_3O_4 electrochemical pathway. The first discharge capacity is about 1116 $mAhg^{-1}$, which is larger than the theoretical values (890 $mAhg^{-1}$). This is usually attributed to the formation of a solid electrolyte interphase (SEI) layer[16]. A relatively low irreversible capacity loss (25%) occurs for the first charging curve at 3.0 V due to the transformation of Co_3O_4 into CoO. Note that after the 2nd cycle there is no obvious performance degradation. The cycling performance together with the Coulombic efficiency of the sample is depicted in Figure 4b. As-prepared CoNs exhibit excellent cyclic capacity retention with a stable capacity. Even after 50 charge-discharge cycles, a reversible capacity as high as 864 $mAhg^{-1}$ can still be retained. This value can be comparative to the theoretical values (890 $mAhg^{-1}$) and is ~2.3 times larger than the theoretical capacity of graphite. In addition, our samples also show much improved rate capabilities, as shown in Figure 4c. CoNs maintain high capacity of ~700 $mAhg^{-1}$ when the current density was increased to 2C. Even at a much larger current density of 5C, our products still show a considerable reversible capacity of 261 $mAhg^{-1}$. It further indicates that the present nanocages are beneficial for the improvement of Co_3O_4 anode materials.

Discussion

The excellent electrochemical performance of CoNs is believed to originate from their unique structural features. Firstly, the crystal plane effect plays the important role, similar to the case of mesoporous NiO nanosheets with highly exposed (110) planes[25]. In our case, (110) planes are also dominantly exposed, which will result in more cobalt atoms on the surfaces of Co_3O_4 crystals when compared with (111) and (001) facets. As illustrated in Figure 5a, 2.5 Co^{2+} and 2 Co^{3+} belong to (110) facets, while only 1.875 Co^{2+} (Fig. 5b) and 1 Co^{2+} (Fig. 5c) are present in (111) and (001) facets, respectively. Furthermore, the analysis of Co_3O_4 surface electronic states[18] based on the first principle calculations testifies that (110) surface terminations enable partial metallization of Co_3O_4 crystals. It will

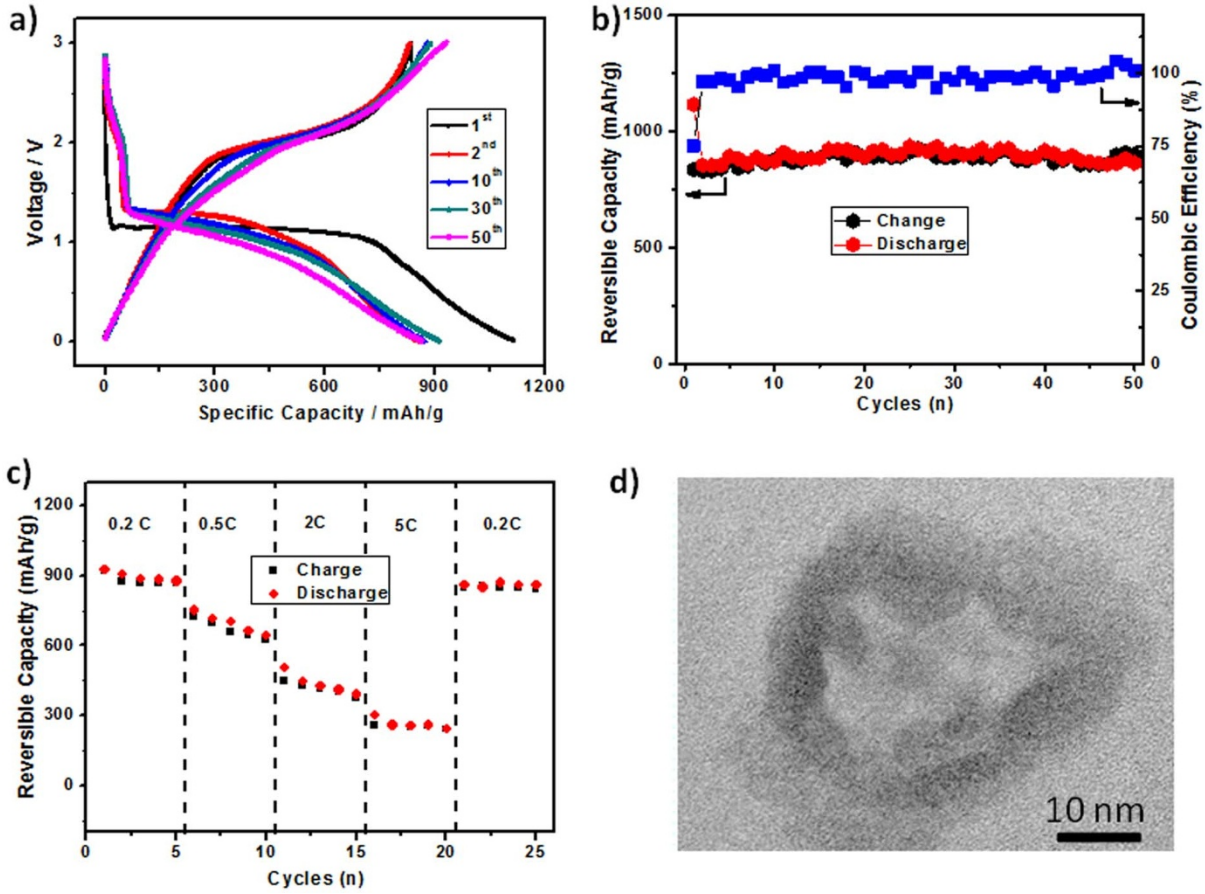

Figure 4 | Electrochemical characterizations and Shape changes during the charge/discharge process. (a) Discharge-charge voltage profiles of CoNs at a current density of 0.2 C. (b) Cycling performance and Coulombic efficiency of CoNs at a current density of 0.2 C. (c) Rate performance of CoNs at different current density, (d) TEM image of CoNs electrodes taken from fully discharged states after 50 cycles.

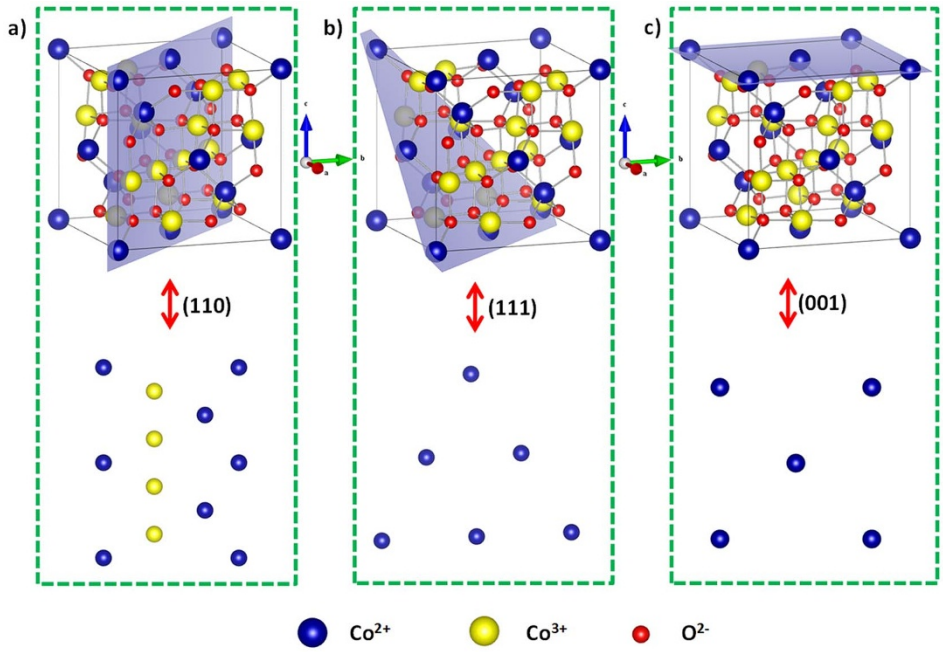

Figure 5 | Theoretical models of the different planes of Co_3O_4. The 3 D and 2 D surface atomic configurations in (a) the (110) plane, (b) the(111) plane, and (c) the (001) plane of Co_3O_4.

lead to enhanced conductivity of Co_3O_4, which is beneficial for the improvement of the electronic transport properties. Secondly, similar to researches on hollow structured anodes, the void space in nanocages can effectively buffer the volume changes during lithium insertion-release[9,13], hence alleviating the problem of pulverization of the electrode materials and improving the cycling performance. TEM characterization of these samples at the fully lithiated states after 50 cycles nicely supports this hypothesis. As shown in Figure 4d, CoNs nanocages still maintain the shape integrity after 50 cycles and their hollow structure is also preserved. It reveals excellent structural stability of CoNs. In addition, similar to the high catalytic activity of nano-catalysts with stepped surfaces[20], the presence of a high density of atomic steps and kinks in the facets may catalytically facilitate the reaction of Li with Co_3O_4. Moreover, the ultrathin nanoshells (2–5 nm) in CoNs not only render a very short transport length for lithium ions during insertion/extraction, but also bring a high surface area, favoring a high rate performance[26–36]. The above synergetic effects peculiar to nanocages are responsible for the excellent electrochemical performance of the whole electrode.

In summary, Co_3O_4 nanocages with highly exposed {110} facets were successfully fabricated via a one-step solution method. Both densely packed EG on the {100} surfaces and bubble templates play the key roles in the formation process. A good cycle performance and much improved rate capability for Co_3O_4 nanocages in LIBs were achieved because of the regarded unique structures: highly exposed {110} planes, high concentration of the stepped surface atoms on surfaces, and the large void interiors.

Methods

Synthesis of Co_3O_4 nanocages with exposed {110} planes. The cobalt precursors were synthesized by a polyol process in hydrothermal conditions. 1 g of $Co(AC)_2{\cdot}4H_2O$ was loaded into a 100 mL stainless steel autoclave, which was then filled with 80 mL ethylene glycol. The autoclave was sealed and maintained at 185°C for 24 h, and then cooled down to room temperature. The precursors were centrifuged, rinsed with distilled water and ethanol several times to remove any impurities. 500 mg of as-prepared precursors were dispersed into a 10 mM H_2O_2 solution (200 ml), and then heated at 80–100°C for 2–5 h. The precursor were centrifuged, rinsed with distilled water and ethanol several times to remove any impurities.

Characterization. The sizes and morphologies of the as-obtained samples were characterized by a field emission scanning electron microscope (FESEM, JSM-4300, JSM-4800, JEOL, Japan), a transmission electron microscope (TEM, JSM-1011, JEOL, Japan), and a high-resolution transmission electron microscope (HRTEM, JSM-3000F, JEOL, Japan) operating at 300 kV. Phases were identified in an X-ray diffractometer (XRD, X-Pert, PANalytic, Netherlands) with Cu Kα radiation (40 kV, 30 mA). The unit cell lattice parameters were obtained by the least-squares fitting method (2θ range, 10–70°) of the d-spacings and the $h\ k\ l$ values. FT-IR spectra were taken on a FTS−45RD Bio-Rad infrared spectrophotometer.

Electrochemical test. For the test of products, the working electrode was prepared by pressing the slurry of 80% sample powders, 10% acetylene black, and 10% PVDF binder (by weight) onto the copper current collector. The electrolyte consisted of a solution of 1 M $LiClO_4$ in ethylene carbonate (EC)/dimethyl carbonate (DMC)/diethyl carbonate (DEC) (1 : 1 : 1, in wt%) obtained from Ferro Corp. A galvanostatic cycling test of the assembled cells was carried out on an charge-discharge unit (Hokuto Denko Co., Ltd.).

1. Yang, H. G., Sun, C. H., Qiao, S. Z., Zou, J., Liu, G., Smith, S. C., Cheng, H. M. & Lv, G. Q. Anatase TiO_2 single crystals with a large percentage of reactive facets. *Nature* **453**, 638 (2008).
2. Liu, S. W., Yu, J. G. & Jaroniec, M. Tunable Photocatalytic Selectivity of Hollow TiO_2 Microspheres Composed of Anatase Polyhedra with Exposed {001} Facets. *J. Am. Chem. Soc.* **132**, 11914 (2010).
3. Wang, X. L., He, H., Chen, L. Y., Zhao, J. Q. & Zhang, X. Y. Anatase TiO_2 hollow microspheres with exposed {001} facets: Facile synthesis and enhanced photocatalysis. *Appl. Surf. Sci.* **258**, 5863 (2012).
4. Xie, S. F., Han, X. G., Kuang, Q., Fu, J., Zhang, L., Xie, Z. X. & Zheng, L. S. Solid state precursor strategy for synthesizing hollow TiO_2 boxes with a high percentage of reactive {001} facets exposed. *Chem. Commun.* **47**, 6722 (2011).
5. Jin, M. S., Zhang, H., Xie, Z. X. & Xia, Y. N. Palladium Concave Nanocubes with High-Index Facets and Their Enhanced Catalytic Properties. *Angew. Chem. Int. Ed.* **50**, 7850 (2011).
6. Xie, X., Li, Y., Liu, Z. Q., Haruta, M. & Shen, W. Low-temperature oxidation of CO catalysed by Co_3O_4 nanorods. *Nature* **458**, 746 (2009).
7. Xiao, X., Liu, X., Zhao, H., Chen, D., Liu, F., Xiang, J., Hu, Z. & Li, Y. Facile Shape Control of Co_3O_4 and the Effect of the Crystal Plane on Electrochemical Performance. *Adv. Mater.* **24**, 5762 (2012).
8. Wang, Y., Zhang, H. J., Wei, J., Wong, C. C., Lin, J. Y. & Borgna, A. Crystal-match guided formation of single-crystal tricobalt tetraoxygen nanomesh as superior anode for electrochemical energy storage. *Energ. Environ. Sci.* **4**, 1845 (2011).
9. Koo, B., Xiong, H., Slater, M. D., Prakapenka, V. B., Balasubramanian, M., Podsiadlo, P., Johnson, C. S. & Rajh, T. Hollow Iron Oxide Nanoparticles for Application in Lithium Ion Batteries. *Nano Lett.* **12**, 2429 (2012).
10. Guo, W., Xue, X., Wang, S., Lin, C. & Wang, Z. L. An Integrated Power Pack of Dye-Sensitized Solar Cell and Li Battery Based on Double-Sided TiO_2 Nanotube Arrays. *Nano Lett.* **12**, 2520 (2012).

11. Caruso, F., Caruso, R. A. & Möhwald, H. Nanoengineering of inorganic and hybrid hollow spheres by colloidal templating. *Science* **282**, 1111 (1998).
12. Wang, X., Liao, M. Y., Zhong, Y. T., Zheng, J. Y., Tian, W., Zhai, T. Y., Zhi, C. Y., Ma, Y., Yao, J. N., Bando, Y. & Golberg, D. ZnO Hollow Spheres with Double-Yolk Egg Structure for High-Performance Photocatalysts and Photodetectors. *Adv. Mater.* **24,** 3421 (2012).
13. Wang, X., Tian, W., Zhai, T. Y., Zhi, C. Y., Bando, Y. & Golberg, D. Cobalt(II,III) oxide hollow structures: fabrication, properties and applications. *J Mater. Chem.* **22**, 23310 (2012).
14. Wang, X., Wu, X., Guo, Y., Zhong, Y., Cao, X., Ma, Y. & Yao, J. N. Synthesis and Lithium Storage Properties of Co_3O_4 Nanosheet-Assembled Multishelled Hollow Spheres. *Adv. Funct. Mater.* **20**, 1680 (2010).
15. Wang, X., Yu, L., Wu, X. L., Guo, Y. G., Ma, Y. & Yao, J. Synthesis of Single-Crystalline Co_3O_4 Octahedral Cages with Tunable Surface Aperture and Their Lithium Storage Properties. *J. Phys. Chem. C* **113**, 15553 (2009).
16. Zhong, Y., Wang, X., Jiang, K., Zheng, J. Y., Guo, Y., Ma, Y. & Yao, J. A facile synthesis and lithium storage properties of Co3O4–C hybrid core-shell and hollow spheres. *J. Mater. Chem.* **21**, 17998 (2011).
17. Hu, L., Peng, Q. & Li, Y. Communication Selective Synthesis of Co_3O_4 Nanocrystal with Different Shape and Crystal Plane Effect on Catalytic Property for Methane Combustion. *J. Am. Chem. Soc.* **130**, 16136 (2008).
18. Chen, J. & Selloni, A. Electronic states and magnetic structure at the Co_3O_4(110) surface: A first-principles study. *Phys. Rev. B* **85**, 085306 (2012).
19. Xu, X. L., Chen, Z. H., Li, Y., Chen, W. K. & Li, J. Q. Bulk and surface properties of spinel Co_3O_4 by density functional calculations. *Surf. Sci.* **603**, 653 (2009).
20. Fujita, T., Guan, P., McKeena, K., Lang, X. Y., Hirata, A., Zhang, L., Tokunaga, T., Arai, S., Yamamoto, Y., Tanaka, N., Ishikawa, Y., Asao, N., Yamamoto, Y., Erlebacher, J. & Chen, M. Atomic origins of the high catalytic activity of nanoporous gold. *Nat. Mater.* **11**, 775 (2012).
21. Molina, L. M. & Hammer, B. Theoretical study of CO oxidation on Au nanoparticles supported by MgO"100. *Phys. Rev. B* **69**, 155424 (2004).
22. Hvolbæk, B., Janssens, T. V. W., Clausen, B. S., Falsig, H., Christensen, C. H. & Nøskov, J. K. Catalytic activity of Au nanoparticles. *Nano Today* **2**, 14 (2007).
23. Banfield, J. F., Welch, S. A., Zhang, H., Ebert, T. T. & Penn, R. L. Aggregation-Based Crystal Growth and Microstructure Development in Natural Iron Oxyhydroxide Biomineralization Products. *Science* **289**, 751 (2000).
24. Schliehe, C., Juarez, B. H., Pelletier, M., Jander, S., Greshnykh, D., Nagel, M., Meyer, A., Foerster, S., Kornowski, A., Klinke, C. & Weller, H. Ultrathin PbS Sheets by Two-Dimensional Oriented Attachment. *Science* **329**, 550 (2010).
25. Su, D., Ford, M. & Wang, G. Mesoporous NiO crystals with dominantly exposed {110} reactive facets for ultrafast lithium storage. *Sci. Rep.* **2**, 924 (2012).
26. Guo, Y. G., Hu, J. S. & Wan, L. J. Nanostructured Materials for Electrochemical Energy Conversion and Storage Devices. *Adv. Mater.* **20**, 2878 (2008).
27. Liu, Z., Zhan, Y., Moldovan, S., Gharbi, M., Song, L., Shi, G., Ma, L., Zhao, S., Huang, J., Vajtai, R., Banhart, F., Sharma, P., Lou, J. & Ajayan, P. M. Anomalous high capacitance in a coaxial single nanowire capacitor. *Nature Commu.* **3**, 879 (2012).
28. Hao, F., Dong, P., Zhang, J., Zhang, Y., Loya, P., Hauge, R. H., Li, J., Lou, J. & Lin, H. High Electrocatalytic Activity of Vertically Aligned Single-Walled Carbon Nanotubes towards Sulfide Redox Shuttles. *Sci. Rep.* **2**, 368 (2012).
29. Wang, X. *et al.* Revealing the conversion mechanism of CuO nanowires during lithiation–delithiation by in situ transmission electron microscopy. *Chem. Commun.* **48**, 4812 (2012).
30. Guan, H., Wang, X., Chen, S., Bando, Y. & Golberg, D. Coaxial Cu-Si@C array electrodes for high-performance lithium ion batteries. *Chem. Commun.* **47**, 12098 (2011).
31. Guan, H., Wang, X., Li, H., Zhai, T., Bando, Y. & Golberg, D. CoO octahedral nanocages for high-performance lithium ion batteries. *Chem. Commun.* **48**, 4878 (2012).
32. Wang, X. *et al.* Multishelled Co_3O_4-Fe_3O_4 hollow spheres with even magnetic phase distribution: Synthesis, magnetic properties and their application inwater treatment. *J. Mater. Chem.* **21**, 17680 (2011).
33. Liu, D. *et al.* Ultrathin nanoporous Fe_3O_4–carbon nanosheets with enhanced supercapacitor performance. *J. Mater. Chem. A* **1**, 1952 (2013).
34. Wang, X., Tian, W., Liu, D., Zhi, C., Bando, Y. & Golberg, D. Unusual formation of α-Fe_2O_3 hexagonal nanoplatelets in N-doped sandwiched graphene chamber for high-performance lithium-ions batteries. *Nano Energy* **2**, 257 (2013).
35. Nethravathi, C. *et al.* N-Doped Graphene–VO_2(B) Nanosheet-Built 3D Flower Hybrid for Lithium Ion Battery. *Acs Appl. Mater. Interfaces* **5**, 2708 (2013).
36. Wang, X., Guan, H., Chen, S., Li, H., Zhai, T., Tang, D., Bando, Y. & Golberg, D. Self-stacked Co_3O_4 nanosheets for high-performance lithium ion batteries. *Chem. Commun.* **47**, 12280 (2011).

Acknowledgements

This work was supported by the World Premier International (WPI) Research Center on Materials Nanoarchitectonics (MANA), MEXT, Japan. This work is also supported by the NIMS International Center for Young Scientists (ICYS) program. The authors thank Dr. Wei Yi for valuable discussions.

Author contributions

D. Liu, X. Wang performed experiments and testing. X. Wang, D. Liu and D. Golberg designed the experiments, discussed the results and co-wrote the manuscript. All authors discussed the results and commented on the manuscript.

Additional information

Supplementary information accompanies this paper at http://www.nature.com/scientificreports

Competing financial interests: The authors declare no competing financial interests.

How to cite this article: Liu, D.Q. *et al.* Co_3O_4 nanocages with highly exposed {110} facets for high-performance lithium storage. *Sci. Rep.* **3**, 2543; DOI:10.1038/srep02543 (2013).